  Bull. Chem. Soc. Jpn., 55, 1447—1453 (1982)

Reactivity of Fe_2O_3 and Fe_2O_3-Al_2O_3 Mixture for Reduction of SO_2 with CO

Tadao Ishii,* Ryusaburo Furuichi, and Koji Shikano

Department of Applied Chemistry, Faculty of Engineering, Hokkaido University, Kita-ku, Sapporo 060

(Received August 31, 1981)

Catalytic reactivities of α-Fe_2O_3 powder (−200 mesh) and a α-Fe_2O_3–γ-Al_2O_3 powder mixture prepared by mechanical mixing, which were preheated at 360—700 °C, were studied for the reduction of SO_2 with CO by means of both a reaction gas-chromatographic technique using CO, SO_2, and 2CO–SO_2 pulses and the powder X-ray analysis. The reactivity of Fe_2O_3 decreases with increasing preheating temperature, which is explained on the basis of redox reactions between Fe_2O_3 and nascent (Fe_3O_4): $6Fe_2O_3+2CO \rightarrow 4(Fe_3O_4)+2CO_2$ and $4(Fe_3O_4)+SO_2 \rightarrow 6Fe_2O_3+1/2S_2$. It is considered that the reactivity of Fe_2O_3 is attributable to the activity of (Fe_3O_4). The lifetime of active (Fe_3O_4) is within about 1 min, and the activity and lifetime of (Fe_3O_4) is increased by interfacial reaction between Fe_2O_3 and Al_2O_3 at 700 °C. The activity maximum in the Fe_2O_3-Al_2O_3 system preheated at 700 °C is attained at 70—75 wt% Fe_2O_3.

The catalytic reduction of sulfur dioxide by carbon monoxide has been extensively investigated. It is generally accepted that the reduction proceeds in the range of about 300 to 600 °C in the following way:

$$SO_2 + 2CO \longrightarrow 2CO_2 + 1/2S_2, \quad (1)$$

$$1/2S_2 + CO \longrightarrow COS. \quad (2)$$

Many catalysts, such as metals, metal oxides, and their mixtures, have been used in the study. Few papers have been published on the use of Fe_2O_3 for preparing the catalyst. Khalafalla *et al.*[1–3] used a catalyst prepared by reducing mixtures of hematite and γ-Al_2O_3 at 600 °C for 1 h with H_2. The hematite constituent of the catalyst was completely reduced to iron. Clay and Lynn[4] reported that iron oxide supported on alumina is a promising catalyst/adsorbent for use in the simultaneous removal of NO_x and SO_x from power plant stack gases. Iron oxide is converted to the iron(II) state, and SO_2 is removed as iron(II) sulfide or sulfate. Kasaoka *et al.*[5] used the coprecipitated metal oxides, Fe_2O_3–Al_2O_3, Fe_2O_3–Cr_2O_3, Fe_2O_3–CuO–Al_2O_3, and Fe_2O_3–Cr_2O_3–Al_2O_3, which were reduced with H_2 at 550 °C. However, studies on catalysts prepared by mechanically mixing Fe_2O_3 and metal oxide powders are rarely found for the SO_2–CO reaction.

In a previous work,[6] Ishii *et al.* examined the reactivity of powder mixtures of α-Fe_2O_3 and metal oxide, α-Al_2O_3, γ-Al_2O_3, MgO, or CaO, on the basis of their catalytic behavior, in the reduction of SO_2 with CO at 300 °C, as characterized by means of reaction gas-chromatography and X-ray analysis. A maximum catalytic activity for reaction (1) was obtained at a specific mixing ratio for each mixture. In a pure pulse of CO, Fe_2O_3 was easily reduced to Fe_3O_4, but in a mixed pulse of $2CO+SO_2$, no change of Fe_2O_3 resulted. This behavior was discussed in connection with the redox reaction between Fe_2O_3 and (Fe_3O_4) in the following way:

$$6Fe_2O_3 + 2CO \longrightarrow 4(Fe_3O_4) + 2CO_2, \quad (3)$$

$$4(Fe_3O_4) + SO_2 \longrightarrow 6Fe_2O_3 + 1/2S_2, \quad (4)$$

where (Fe_3O_4) means nascent Fe_3O_4. The unique catalytic behavior of this powder mixture appeared to be related to a reaction at the interface between Fe_2O_3 and oxide, which occurred during preheating the mixture.

In the present paper, on the basis of reactions (3) and (4) proposed, reactivities of α-Fe_2O_3 powder and a α-Fe_2O_3–γ-Al_2O_3 powder mixture prepared by mechanical mixing, which were preheated at various temperatures, were studied in detail for the reduction of SO_2 with CO.

Experimental

Materials. Reagent grade commercial α-Fe_2O_3 (Kanto) and γ-Al_2O_3 (Merck), which are hereinafter written as Fe_2O_3 and Al_2O_3, respectively, were used without further purification. All starting materials were ground so as to pass a 200 mesh sieve. The powder mixture was prepared by mixing Fe_2O_3 and Al_2O_3 powders for 2 h by means of a rotating-V-type micro mixer (Tsutsui Rikagaku). Commercial SO_2 (Teikoku), CO (Nissan), and CO_2 (Hokusan) were used without further purification.

Preliminary Calcining (Preheating). Prior to reactivity tests, powder samples were preheated at various temperatures, 360, 600, and 700 °C, for 1 h in a flowing He (25 cm³/min) in the same reactor as was used for testing the reactivity. It was confirmed from X-ray analysis that, by these preheating processes, neither new products are formed in the Fe_2O_3–Al_2O_3 system nor any change in γ-Al_2O_3 is shown.

Apparatus and Procedures. A pulse method using a reaction gas-chromatograph (Hitachi, K-23 type) was applied to study of the adsorption of SO_2 and CO and of the catalytic reduction of SO_2 with CO. The standard experimental conditions were as follows: pulse interval, 25 min; pulse volume, 0.5 cm³ of SO_2 and 1 cm³ of CO; carrier gas, 25 cm³/min of He; reaction temperature, 360±5 °C; reactor, a quartz tube of 5.5 mm diameter; separating column, a stainless steel tube of 3 mm diameter; packing, Porapak-QS 80—100 mesh (Gasukuro Kogyo) at 60 °C. Eighty mg of a Fe_2O_3–Al_2O_3 powder mixture with a mixing ratio in the range 0—100% and 24—80 mg of Fe_2O_3 were packed in the reactor. Both sides of these packed samples were fixed by glass wool. A glass injection-syringe of 1 cm³ was used for injecting SO_2 and CO gases into the reactor. In order to inject the mixture of CO (1 cm³) and SO_2 (0.5 cm³), these gases were simultaneously injected by use of two syringes. After preheating the catalyst sample, the temperature of the reactor was adjusted to the reaction temperature 360 °C without lowering the sample temperature to room temperature. The time required for lowering the preheating temperature (600—700 °C) to the reaction

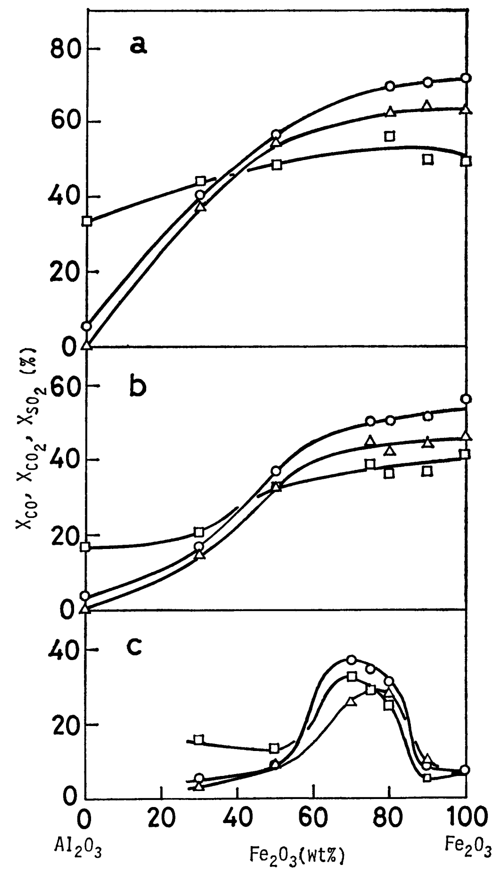

Fig. 1. Per cent conversions of CO and SO_2 (X_{CO} and X_{SO_2}), and % formation of CO_2 (X_{CO_2}) in $2CO+SO_2$ pulse for Fe_2O_3–Al_2O_3 systems with various mixing ratios and preheating temperatures.
Preheating temperature; (a): 360 °C, (b): 600 °C, (c): 700 °C. ○: X_{CO}, △: X_{CO_2}, □: X_{SO_2}.

temperature 360 °C was about 20—30 min. X-Ray analysis of samples before and after tests was carried out with a diffractometer (Geigerflex type-2004, Rigaku Denki) under the conditions: Co target, Fe filter, 35 kV, 10 mA, count full scale 1000 c/s, and scanning speed 1°/min.

Conversion of CO and SO_2 (X_{CO} and X_{SO_2}) and Formation of CO_2 (X_{CO_2}). For pulses of CO or SO_2 alone, areas of chromatographic peaks of CO, SO_2, and CO_2 at the outlet of reactor, relative to those for a blank test with no powder sample, were used for the determination of per cent conversions of CO (X_{CO}) and SO_2 (X_{SO_2}) and per cent formation of CO_2 (X_{CO_2}). The blank test for X_{CO_2} was carried out by using CO_2 gas.

For pulses of the mixture of CO and SO_2 ($2CO+SO_2$ pulse), the area of chromatographic peak of CO_2 at the outlet of reactor, relative to that of a blank test carried out using $2CO_2+SO_2$ pulse instead of $2CO+SO_2$ pulse, was used for the determination of per cent formation of CO_2 (X_{CO_2}) on the basis of reaction (1). Per cent conversions of CO (X_{CO}) and SO_2 (X_{SO_2}) were determined in the same way as for pulses of CO or SO_2 alone. Unless otherwise noted, arithmetic mean of five pulses was used as the value of X_{CO}, X_{SO_2}, or X_{CO_2}.

Results and Discussion

Fe_2O_3–Al_2O_3 System. Various pulse tests were carried out for the Fe_2O_3–Al_2O_3 system.

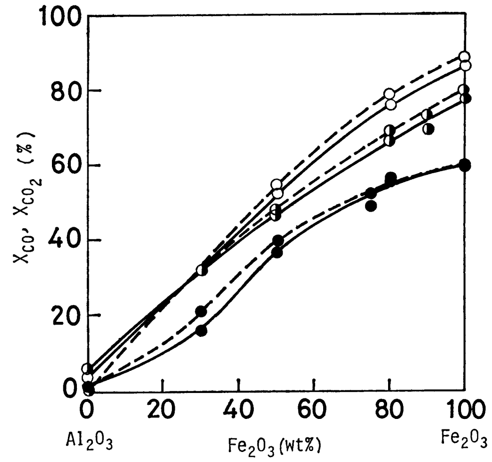

Fig. 2. Per cent conversion of CO (X_{CO}) and formation of CO_2 (X_{CO_2}) in CO pulse for Fe_2O_3–Al_2O_3 systems with various mixing ratios and preheating temperatures.
Preheating temperature: ○: 360 °C, ◑: 600 °C, ●: 700 °C. ——: X_{CO}, ----: X_{CO_2}.

$2CO+SO_2$ Pulse: Figures 1(a)—(c) show per cent conversions of CO and SO_2 (X_{CO} and X_{SO_2}) and per cent formation of CO_2 (X_{CO_2}) in $2CO+SO_2$ pulse for the Fe_2O_3–Al_2O_3 systems with various mixing ratios (wt% of Fe_2O_3). (a) is the result of the sample preheated at 360 °C. The value of X_{CO} increases from 4.8% for Al_2O_3 alone (adsorption of CO) to 71.5% for Fe_2O_3 alone with increasing Fe_2O_3 content. The value of X_{CO_2} increases similarly to X_{CO}, but it is generally several per cents lower than the X_{CO} value. This seems to be due to occurrence of a side reaction such as reaction (2). Al_2O_3 alone does not show any activity for reaction (1). The value of X_{SO_2} increases from 33.2% for Al_2O_3 alone (adsorption of SO_2) to 49.2% for Fe_2O_3 alone with increasing Fe_2O_3 content. The fact that the X_{SO_2} value for Fe_2O_3 alone is lower than that of X_{CO_2} may be due to a lowering of activity of nascent (Fe_3O_4) on reaction (4) as will be considered later. Compared with (a), all the values in (c) for the samples preheated at 700 °C are significantly low, and the maximum X_{CO}, X_{SO_2}, and X_{CO_2} values are attained at their respective specific mixing ratios at about 70—75 wt% of Fe_2O_3 contents. The samples preheated at 600 °C on (b) show an intermediate behavior between (a) and (c).**

CO Pulse: Figure 2 shows the result of a CO pulse for the Fe_2O_3–Al_2O_3 systems with various mixing ratios and preheating temperatures. The value of X_{CO} increases in an approximately linear relationship with increasing ratio of Fe_2O_3, but it decreases with increasing preheating temperature. CO_2 is formed on all of samples except for Al_2O_3 alone, and X_{CO_2} is approximately the same as X_{CO}. These results show occurrence of reaction (5) without adsorption of CO:

$$3Fe_2O_3 + CO \longrightarrow 2F_3O_4 + CO_2. \qquad (5)$$

** In a previous paper,[6] an activity maximum was attained at 80—90 wt% Fe_2O_3 preheated at 600 °C. This is probably due to the use of different lot No. of commercial Fe_2O_3 sample and different reaction temperature (300 °C).

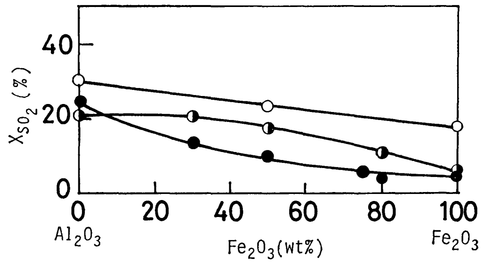

Fig. 3. Per cent conversion of SO_2 (X_{SO_2}) in SO_2 pulse for Fe_2O_3–Al_2O_3 systems with various mixing ratios and preheating temperatures.
Preheating temperature: ○: 360 °C, ◑: 600 °C, ●: 700 °C.

SO_2 Pulse: Figure 3 shows that the value of X_{SO_2} decreases with increasing ratio of Fe_2O_3 and preheating temperature. The values of X_{SO_2} for Al_2O_3 alone and Fe_2O_3 alone are 20—30 and 5—20%, respectively. It is thought that these values of X_{SO_2} may be due to irreversible adsorption of SO_2, because the experiments were carried out at 25-min pulse intervals in a flowing He gas.

Fe_2O_3 System. The effect of Al_2O_3 in the Fe_2O_3–Al_2O_3 systems of Figs. 1 and 2 on the reactions was examined by comparison with the results of the pure Fe_2O_3 system, of which the amounts of Fe_2O_3 correspond to those in the Fe_2O_3–Al_2O_3 systems (*e.g.*, 40 mg Fe_2O_3 corresponds to 50 wt% Fe_2O_3 in the Fe_2O_3–Al_2O_3 system).

$2CO+SO_2$ Pulse: Figures 4(a)—(c) show results of Fe_2O_3 preheated at 360, 600, and 700 °C in the pulse of $2CO+SO_2$, respectively. In the case of (a), the curves of X_{CO} and X_{CO_2} are similar to that in Fig. 1(a). Consequently, it is thought that no cooperative action between Fe_2O_3 and Al_2O_3 takes place during the preheating of the Fe_2O_3–Al_2O_3 system at 360 °C, and the behavior in the Fe_2O_3–Al_2O_3 system of Fig. 1(a) is attributable to that of Fe_2O_3 itself. Khalafalla *et al.*[1] reported that results in the Fe–Al_2O_3 system for reaction (1) are best explained on the basis of a dual-site mechanism with both iron and alumina augmenting their specific-site activities at their interparticle contacts. However, the present results indicate no action of bifunctional catalyst. Furthermore, on the basis of a comparison between X_{CO} or X_{CO_2} of Fig. 1(a) and that of Fig. 4(a), it is considered that there is no problem with respect to the contact between gas and powder arising from the small packing amount of powder used. On the other hand, the value of X_{SO_2} greatly differs from that in the Fe_2O_3–Al_2O_3 system, especially in the low Fe_2O_3 content region. This is due mainly to the adsorption of SO_2 on Al_2O_3.

In the case of Fig. 4(c), the curves differ grealty from that in Fig. 1(c). Consequently, it can be considered with regard to the unique catalytic behavior of Fig. 1(c) that some interfacial reactions between Fe_2O_3 and Al_2O_3 occurred during the preheating process at 700 °C. Figure 4(b) shows an intermediate behavior between (a) and (c).

CO Pulse: Figure 5 shows the result of Fe_2O_3 alone with various Fe_2O_3 amounts and preheating temperatures. The results obtained are approximately the same as that of the Fe_2O_3–Al_2O_3 systems in Fig. 2. This means that there is no significant effect of Al_2O_3 on reaction (5) in the Fe_2O_3–Al_2O_3 systems for all

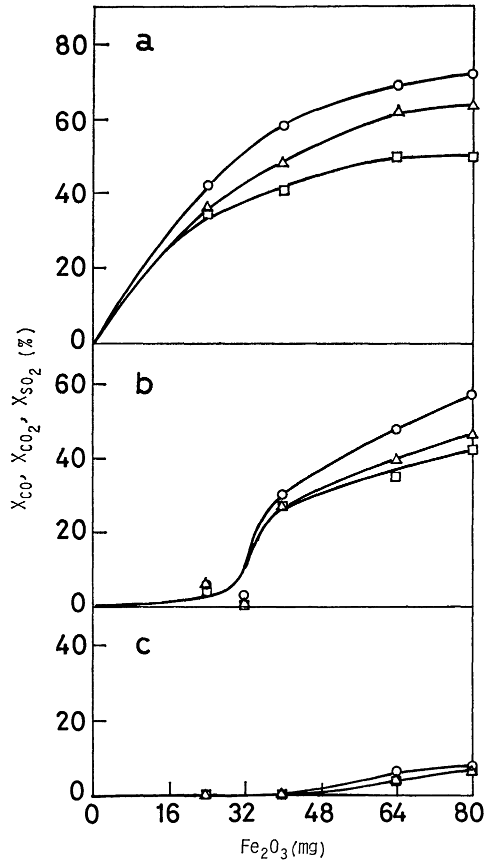

Fig. 4. Per cent conversions of CO and SO_2 (X_{CO} and X_{SO_2}),a nd % formation of CO_2 (X_{CO_2}) in $2CO+SO_2$ pulse for Fe_2O_3 systems with various Fe_2O_3 amounts and preheating temperatures.
Preheating temperature: (a): 360 °C, (b): 600 °C, (c): 700 °C. ○: X_{CO}, △: X_{CO_2}, □: X_{SO_2}.

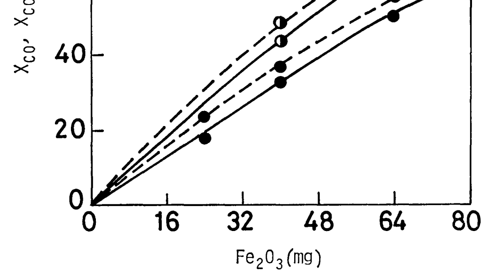

Fig. 5. Per cent conversion of CO (X_{CO}) and % formation of CO_2 (X_{CO_2}) in CO pulse for Fe_2O_3 systems wit hvarious Fe_2O_3 amounts and preheating temperatures.
Preheating temperature: ◑: 600 °C, ●: 700 °C.
——: X_{CO}, ----: X_{CO_2}.

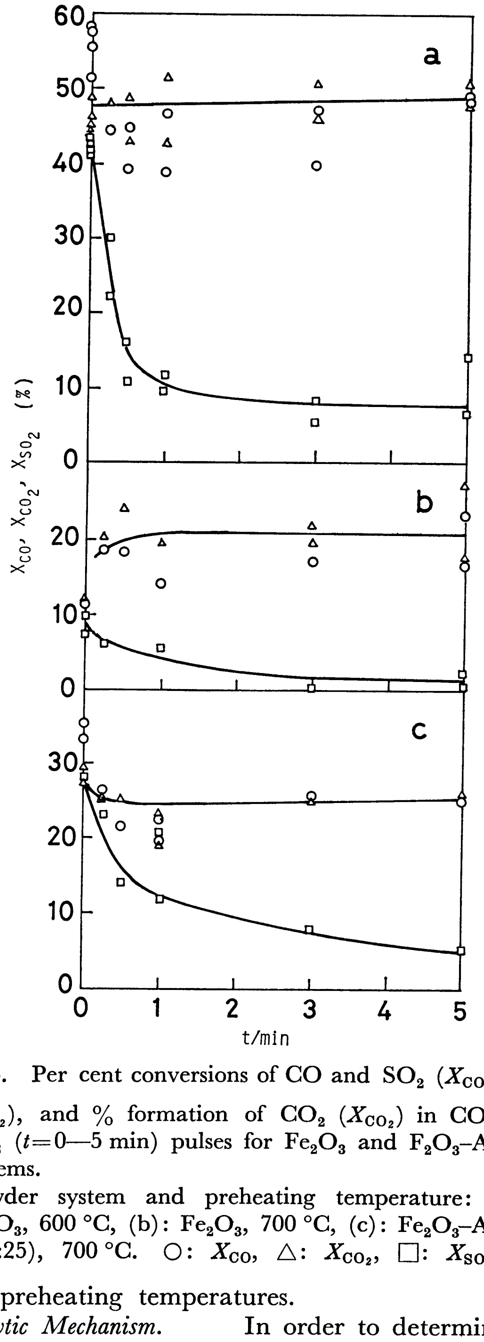

Fig. 6. Per cent conversions of CO and SO_2 (X_{CO} and X_{SO_2}), and % formation of CO_2 (X_{CO_2}) in $CO \xrightarrow{t} SO_2$ (t=0—5 min) pulses for Fe_2O_3 and F_2O_3–Al_2O_3 systems.
Powder system and preheating temperature: (a): Fe_2O_3, 600 °C, (b): Fe_2O_3, 700 °C, (c): Fe_2O_3–Al_2O_3 (75:25), 700 °C. ○: X_{CO}, △: X_{CO_2}, □: X_{SO_2}.

of the preheating temperatures.

Catalytic Mechanism. In order to determine, on the basis of reactions (3) and (4) which are proposed in the previous paper,[6] mechanism of the reduction of SO_2 with CO for the Fe_2O_3 and Fe_2O_3–Al_2O_3 systems, a pulse method (with varying pulse intervals), different from the above-described, was applied, and the composition of samples before and after the pulse experiment was identified by X-ray analysis.

$CO \xrightarrow{t} SO_2$ Pulse: Figures 6(a)—(c) show results of experiments where the first CO pulse was injected, followed by a SO_2 pulse, with varying pulse intervals t (min). Figure 6(a) shows that, for Fe_2O_3 preheated at 600 °C, reaction (3) proceeds with approximately constant value of X_{CO_2} regardless of t. The value of X_{CO} is similar to that of X_{CO_2}, although the data show some scatter (the curve of X_{CO} is not shown). In contrast to these results, the curve of X_{SO_2} decreases rapidly within t=1 min and then approaches the values

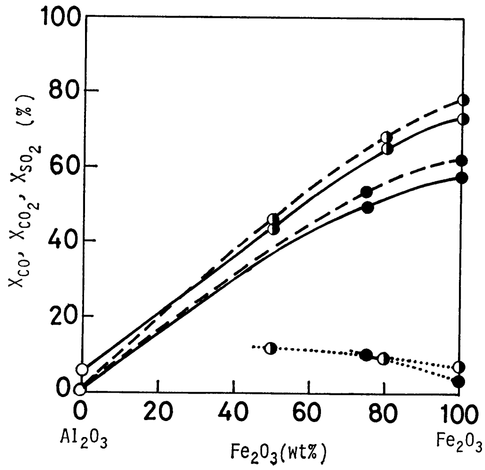

Fig. 7. Per cent conversions of CO and SO_2 (X_{CO} and X_{SO_2}), and % formation of CO_2 (X_{CO_2}) in $CO \times 5 \xrightarrow{t} SO_2 \times 5$ (t=25 min) pulse for Fe_2O_3–Al_2O_3 systems with various mixing ratios and preheating temperatures.
Preheating temperature: ◑: 600 °C, ●: 700 °C.
——: X_{CO}, – – –: X_{CO_2}, ······: X_{SO_2}.

of X_{SO_2} for Fe_2O_3 (in Fig. 3) and Fe_3O_4 (commercial reagent) in the SO_2 pulse. From these results, it is thought that the activity of the nascent (Fe_3O_4) for reaction (4) decreases rapidly within 1 min of t. Figure 6(b) shows the result of Fe_2O_3 preheated at 700 °C. A behavior similar to (a) is shown, but all values of X_{CO}, X_{CO_2} and X_{SO_2} are significantly lower than (a). This is assumed to be due to a decrease in the reactivity of Fe_2O_3 caused by the preheating at higher temperature.

Figure 6(c) shows the result of the Fe_2O_3–Al_2O_3 (75:25) system preheated at 700 °C. The vaule of X_{SO_2} generally increases compared with (b), and the decreasing tendency of X_{SO_2} curve is mild compared with (a), while the values of X_{CO} and X_{CO_2} do not increase very much compared with (b) except for that of t=0 min. These probably mean the reactivity of nascent (Fe_3O_4) for reaction (4) become high and stable with addition of Al_2O_3 with Fe_2O_3, which results from interfacial reaction between Fe_2O_3 and Al_2O_3 caused by the preheating treatment at 700 °C.

$CO \times 5 \xrightarrow{t} SO_2 \times 5$ (t=25 min) Pulse: Figure 7 shows that, for the Fe_2O_3–Al_2O_3 system preheated at 600 and 700 °C, the first five CO pulses (25 min intervals) are injected, followed by five SO_2 pulses (25 min intervals) with 25 min of t. The curves of X_{CO} and X_{CO_2} are similar to that of Fig. 2, but the values of X_{SO_2} are greatly lower than that of Fig. 1, and approximately the same as that of the SO_2 pulse in Fig. 3. This means that the active nascent (Fe_3O_4) was changed to inactive Fe_3O_4 during the interval of 25 min and that the activity of (Fe_3O_4) for reaction (4) disappeared.

$SO_2 \xrightarrow{t} CO$ (t=5 min) Pulse: For the samples of Fe_2O_3 preheated at 360 and 600 °C, first a SO_2 pulse was injected, followed by a CO pulse with t of 5 min. The values of X_{CO_2}, X_{CO}, and X_{SC_2} were 0, 0.2, and 11.4% for the 360 °C preheating and 0, 1.1, and 4.6%

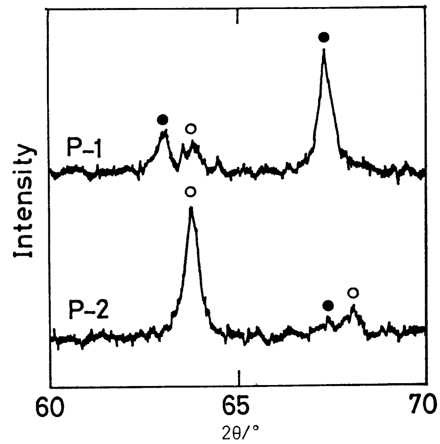

Fig. 8. X-Ray diffraction patterns after pulse experiments for Fe_2O_3 system preheated at 360 °C.
P-1: Fe_2O_3 in CO pulse, P-2: Fe_2O_3 in $2CO+SO_2$ pulse. ○: Fe_2O_3, ●: Fe_3O_4.

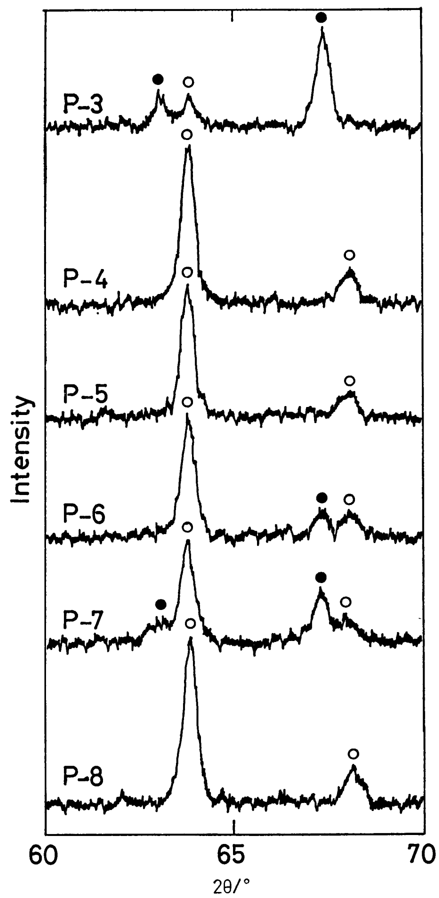

Fig. 9. X-Ray diffraction patterns after pulse experiments for Fe_2O_3 and Fe_2O_3-Al_2O_3 systems preheated at 600 °C.
P-3: Fe_2O_3 in CO pulse, P-4: Fe_2O_3 in $2CO+SO_2$ pulse, P-5: Fe_2O_3-Al_2O_3 (80:20) in $2CO+SO_2$ pulse, P-6: Fe_2O_3 in $CO \xrightarrow{t} SO_2$ (t=0.25 min) pulse, P-7: Fe_2O_3 in $CO \xrightarrow{t} SO_2$ (t=5 min) pulse, P-8: Fe_2O_3 in $SO_2 \xrightarrow{t} CO$ (t=5 min) pulse. ○: Fe_2O_3, ●: Fe_3O_4.

for the 600 °C preheating, respectively. These mean that reaction (5) is hindered by the SO_2 adsorbed on the surface of Fe_2O_3 particle and that the surface reaction between adsorbed SO_2 and gas phase CO did not occur.

X-Ray Analysis: On the basis of the results described above, it is considered that the reactivity of Fe_2O_3 for the reduction of SO_2 to S_2 is governed by the activity and lifetime of nascent (Fe_3O_4) with respect to the redox reactions (3) and (4). In order to confirm this consideration, X-ray analyses of samples were done after these experiments. These results are partly shown in Figs. 8—10 by using diffraction patterns at 2θ=60—70° (Co $K\alpha$). The ASTM cards (13—534 and 11—614) show that 2θ=63.8 and 68.0° (I/I_o=60 and 16) correspond to α-Fe_2O_3 and that 2θ=63.0 and 67.3° (I/I_o=60 and 85) correspond to Fe_3O_4.

Figure 8 shows the result of Fe_2O_3 preheated at 360 °C. Pattern 1 (noted as P-1) in CO pulse shows the formation of Fe_3O_4 on reaction (5) and the presence of small amounts of α-Fe_2O_3 remaining. P-2 in $2CO+SO_2$ pulse shows Fe_2O_3 with trace amounts of Fe_3O_4, which resulted from reaction (3) and (4).

Figure 9 shows the result of both the Fe_2O_3 and Fe_2O_3-Al_2O_3 (80:20) systems which were preheated at 600 °C. P-3 in CO pulse for Fe_2O_3 shows a pattern similar to P-1. P-4 in $2CO+SO_2$ pulse for Fe_2O_3 shows Fe_2O_3 formed as a result of reactions (3) and (4). P-5 in $2CO+SO_2$ pulse for the Fe_2O_3-Al_2O_3 system is the same as P-4. P-6 in $CO \xrightarrow{t} SO_2$ (t=0.25 min) pulse for Fe_2O_3 shows Fe_2O_3 with small amounts of Fe_3O_4. P-7 in $CO \xrightarrow{t} SO_2$ (t=5 min) pulse for Fe_2O_3 shows that Fe_3O_4 increases with increasing t and that active (Fe_3O_4) changes to inactive Fe_3O_4. These results (P-4, P-6, and P-7) support the consideration with Fig. 6(a). P-8 in $SO_2 \xrightarrow{t} CO$ (t=5 min) pulse for Fe_2O_3 shows Fe_2O_3 only, in supports of the consideration with the $SO_2 \xrightarrow{t} CO$ pulse tests shown above.

Figure 10 shows the result of both the Fe_2O_3 and Fe_2O_3-Al_2O_3 (75:25) systems which were preheated at 700 °C. P-9 in CO pulse for Fe_2O_3 shows a pattern similar to P-3. In a comparison of P-1, P-3, and P-9, relative intensities of Fe_2O_3 increase with increasing preheating temperature. This means that the reactivity of Fe_2O_3 decreases with increasing preheating temperature. P-10 in $2CO+SO_2$ pulse for Fe_2O_3 shows Fe_2O_3 only in analogy with P-4. P-11 in $2CO+SO_2$ pulse for the Fe_2O_3-Al_2O_3 system is similar to P-10. P-12 in $CO \xrightarrow{t} SO_2$ (t=0.25 min) pulse for Fe_2O_3 shows Fe_2O_3 only, but P-13 in $CO \xrightarrow{t} SO_2$ (t=5 min) pulse for Fe_2O_3 shows the presence of Fe_3O_4. This means that active (Fe_3O_4) changes to inactive Fe_3O_4 with increasing t, in a similar manner with P-7. P-14 in $CO \xrightarrow{t} SO_2$ (t=0.25 min) pulse for the Fe_2O_3-Al_2O_3 system shows Fe_2O_3 only, but P-15 in $CO \xrightarrow{t} SO_2$ (t=5 min) pulse for the Fe_2O_3-Al_2O_3 system shows the presence of Fe_3O_4 in analogy with P-13.

X-Ray patterns, in $CO\times5 \xrightarrow{t} SO_2\times5$ (t=25 min)

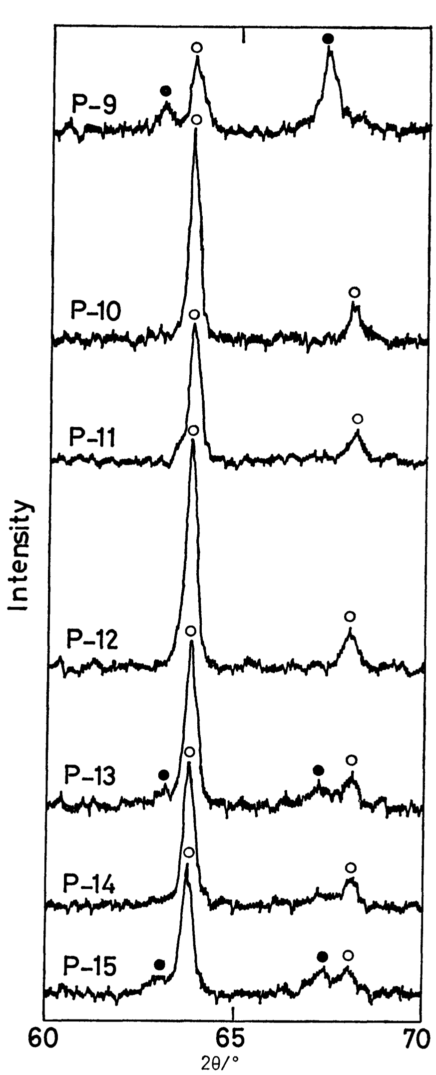

Fig. 10. X-Ray diffraction patterns after pulse experiments for Fe_2O_3 and Fe_2O_3–Al_2O_3 systems preheated at 700 °C.
P-9: Fe_2O_3 in CO pulse, P-10: Fe_2O_3 in $2CO+SO_2$ pulse, P-11: Fe_2O_3–Al_2O_3 (75:25) in $2CO+SO_2$ pulse, P-12: Fe_2O_3 in $CO \xrightarrow{t} SO_2$ (t=0.25 min) pulse, P-13: Fe_2O_3 in $CO \xrightarrow{t} SO_2$ (t=5 min) pulse, P-14: Fe_2O_3–Al_2O_3 (75:25) system in $CO \xrightarrow{t} SO_2$ (t=0.25 min) pulse, P-15: Fe_2O_3–Al_2O_3 (75:25) system in $CO \xrightarrow{t} SO_2$ (t=5 min) pulse. ○: Fe_2O_3, ●: Fe_3O_4.

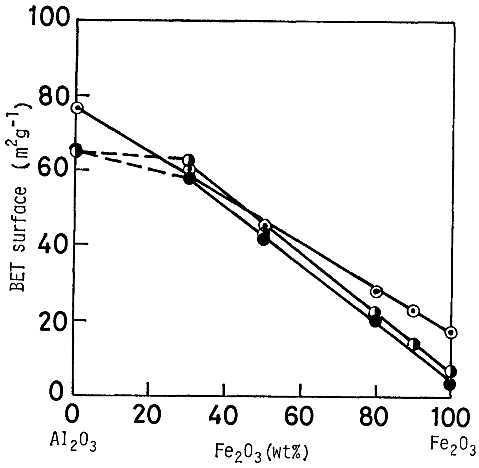

Fig. 11. BET surface of Fe_2O_3–Al_2O_3 systems with various mixing ratios and preheating temperatures. Preheating temperature: ⊙: non-preheating, ◑: 600 °C, ●: 700 °C.

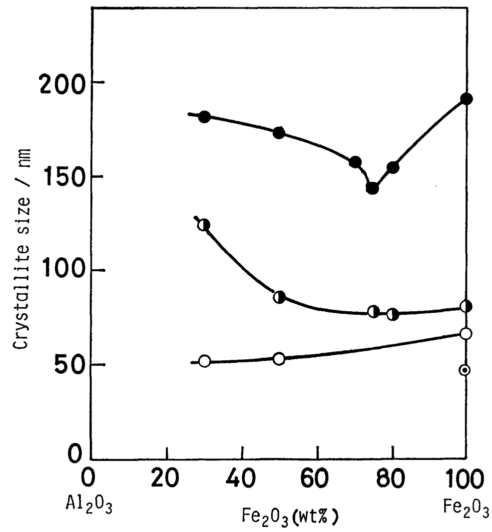

Fig. 12. Crystallite size of Fe_2O_3 (D_{104}) in Fe_2O_3–Al_2O_3 systems with various mixing ratios and preheating temperatures.
Preheating temperature: ⊙: non-preheating, ○: 360 °C, ◑: 600 °C, ●: 700 °C.

pulse, for the same samples with of P-3 and P-5 in Fig. 9 and with P-9 and P-11 in Fig. 10, showed the same results as P-3 and P-9 in CO pulse. These results also support the consideration of $CO \times 5 \xrightarrow{t} SO_2 \times 5$ (t=25 min) pulse in Fig. 7.

In order to test the reactivity of magnetite, pulse tests of $2CO+SO_2$ and SO_2 pulses were carried out for commercial Fe_3O_4 (Kanto) preheated at 360 °C. No reactivity for reaction (1) and no change in X-ray pattern for reaction (4) were shown.

From these discussions described above, the catalytic action may be explained on the basis of redox reaction between Fe_2O_3 and nascent (Fe_3O_4), which has been shown in reactions (3) and (4).

BET Surface and Crystallite Size. In order to examine the effect of Al_2O_3 on the reactivity of Fe_2O_3, some considerations were also attempted. Figure 11 shows the relationship between BET surface and Fe_2O_3 contents for the Fe_2O_3–Al_2O_3 systems with various mixing ratios and preheating temperatures. BET surface decreases with increasing Fe_2O_3 content in approximately a linear relationship. No good correlation is obtained between the reactivity of Fe_2O_3–Al_2O_3 mixture for the reduction of SO_2 (in Fig. 1) and BET surface. This is probably due to the sequence that the BET surface of inactive Al_2O_3 would govern that of the Fe_2O_3–Al_2O_3 mixture.

Figure 12 shows the relationship between the crystallite size of Fe_2O_3 as calculated from Scherrer's equation and the Fe_2O_3 content in the Fe_2O_3–Al_2O_3 system. There are some interesting correlations between the crystallite size and the reactivity behavior in Fig. 1, especially at 700 °C of preheating temperature. If the minimum crystallite size value suggests the maximum distortion of the Fe_2O_3 lattice at 700 °C for preheating, it can be presumed that the occurrence of the maximum peak in Fig. 1(c) may be due to the distortion of the Fe_2O_3 lattice, which results from the interfacial reaction with surface diffusion between Fe_2O_3 and Al_2O_3. Furthermore, it is speculated that the activity of (Fe_3O_4) should be enhanced and the lifetime of active (Fe_3O_4) prologened by the interfacial reaction with Al_2O_3, as indicated by a comparison of Figs. 6(b) and (c).

References

1) S. E. Khalafalla, E. F. Foerster, and L. A. Hass, *Ind. Eng. Chem., Prod. Res. Dev.*, **10**, 133 (1971).

2) S. E. Khalafalla and L. A. Hass, *J. Catal.*, **24**, 115 (1972).

3) L. A. Hass and S. E. Khalafalla, *J. Catal.*, **29**, 264 (1973).

4) D. T. Clay and S. Lynn, *AIChE J.*, **21**, 466 (1975).

5) S. Kasaoka, H. Tsumaki, and T. Kochihira, *Nippon Kagaku Kaishi*, **1973**, 413.

6) T. Ishii, R. Furuichi, and K. Takamatsu, *Nippon Kagaku Kaishi*, **1980**, 1685.